Book Chapter

Design and Parametric Analysis of the Constant Force Characteristics of the Electromagnet for Hydraulic Valves

Wang Ren^{1,2,3}*, Liujie Wu⁴, Wei Zhang⁵, Pengfei Jiang^{1,2,3}, Ziyue Wang^{1,2,3}, Chao Luo^{1,2,3}, Jichang Guo^{1,2,3}, Chang Liu^{1,2,3}, Yaozhong Wei^{1,2,3}, Zhiliang Chen^{1,2,3}, Zongke He^{1,2,3}, Yijie Liu^{1,2,3}, Ting Yu^{1,2,3}, **Yanhe Song^{4*}** and **Bin Yu^{4*}**

¹Coal Mining Research Institute, China Coal Technology and Engineering Group Co., Ltd., Beijing 100013, China

²CCTEG Intelligent Strata Control Technology (Tianjin) Co., Ltd., Tianjin 300392, China

³State Key Laboratory of Intelligent Mining and Strata Control, Beijing 100013, China

⁴School of Mechanical Engineering, Yanshan University, Qinhuangdao 066004, China

⁵Coal Mining Branch, China Coal Research Institute, Beijing 100013, China

*Corresponding Authors: Wang Ren, Coal Mining Research Institute, China Coal Technology and Engineering Group Co., Ltd., Beijing 100013, China

Yanhe Song, School of Mechanical Engineering, Yanshan University, Qinhuangdao 066004, China

Bin Yu, School of Mechanical Engineering, Yanshan University, Qinhuangdao 066004, China

Published March 20, 2025

This Book Chapter is a republication of an article published by Bin Yu, et al. at Processes in November 2024. (Ren, W.; Wu, L.; Zhang, W.; Jiang, P.; Wang, Z.; Luo, C.; Guo, J.; Liu, C.; Wei, Y.; Chen, Z.; et al. Design and Parametric Analysis of the Constant Force Characteristics of the Electromagnet for

Hydraulic Valves. Processes 2024, 12, 2632. https://doi.org/10.3390/pr12122632)

How to cite this book chapter: Wang Ren, Liujie Wu, Wei Zhang, Pengfei Jiang, Ziyue Wang, Chao Luo, Jichang Guo, Chang Liu, Yaozhong Wei, Zhiliang Chen, Zongke He, Yijie Liu, Ting Yu, Yanhe Song, Bin Yu. Design and Parametric Analysis of the Constant Force Characteristics of the Electromagnet for Hydraulic Valves. In: Top 10 Contributions in Process Systems. Hyderabad, India: Academic Reads. 2025.

© The Author(s) 2025. This article is distributed under the terms of the Creative Commons Attribution 4.0 International License (http://creativecommons.org/licenses/by/4.0/), which permits unrestricted use, distribution, and reproduction in any medium, provided the original work is properly cited.

Author Contributions: Conceptualization, W.R., L.W. and Y.S.; methodology, W.R., L.W. and Y.S.; software, W.R., validation, W.R. and Y.S.; formal analysis, W.R., L.W. and Y.S.; resources, L.W.; writing—original draft preparation, W.R., Y.L. and Y.S.; writing—review and editing, W.R., Y.L., T.Y. and Y.S.; visualization, W.R. and W.Z.; supervision, P.J. and B.Y.; project administration, P.J.; funding acquisition, Z.W., C.L. (Chao Luo), J.G., C.L. (Chang Liu), Y.W., Z.C. and Z.H. All authors have read and agreed to the published version of the manuscript.

Funding: This work was funded by the National Natural Science Foundation of China under Grant (52374125, 52304140, 52104162, 52104091, 52304172 and 52304138) and CCTEG Coal Mining Research Institute Science and Technology Innovation Fund (KCYJY-2024-MS-09).

Data Availability Statement: The original contributions presented in this study are included in this paper, and further inquiries can be directed to the corresponding authors.

Conflicts of Interest: Authors Wang Ren, Pengfei Jiang, Ziyue Wang, Chao Luo, Jichang Guo, Chang Liu, Yaozhong Wei,

Zhiliang Chen, Zongke He, Yijie Liu and Ting Yu were employed by the company China Coal Technology and Engineering Group Co., Ltd. and CCTEG Intelligent Strata Control Technology (Tianjin) Co., Ltd. The remaining authors declare that the research was conducted in the absence of any commercial or financial relationships that could be construed as a potential conflict of interest. The companies had no role in the design of the study; in the collection, analyses, or interpretation of data; in the writing of the manuscript, or in the decision to publish the results.

Abstract

The electromagnet is the most used driving device for hydraulic valves; especially the proportional electromagnet with constant force characteristics is the basis for the excellent control performance of hydraulic valves. However, the constant force characteristics of the proportional electromagnet are related to many parameters and are difficult to obtain. In view of the above problems, this paper designs a proportional electromagnet for driving hydraulic valves with the goal of constant force characteristics, with the minimum variance of the output electromagnetic force in the working range as the condition. Firstly, this paper introduces the working principle of proportional electromagnets and establishes the model of electromagnetic force. Then, the influences of the basin bottom radius, the guide angle width and the basin mouth depth on the constant force characteristics of the electromagnet were studied by the finite element method (FEM). Their values are found respectively to give the electromagnet constant force characteristics. Finally, the test bench of the electromagnet was built, and its constant force characteristics and output characteristics were continuously tested. The results show that the test results of the output electromagnet force are highly consistent with the simulation results and have constant force characteristics. Related research deepens the understanding of how the key parameters affect the constant force characteristics, and helps designers optimize these parameters to develop new structures, which have certain practical engineering values.

Keywords

Hydraulic Valve; Proportional Electromagnet; Finite Element Method; Constant Force Characteristics; Parameter Analysis

1. Introduction

A hydraulic valve is a kind of hydraulic component with high power density, which is widely used in a variety of heavy equipment and intelligent equipment [1-4]. Controlling the movement of the valve core to change the working state of the hydraulic valve changes the pressure and flow of the hydraulic system [5,6]. The driving modes of the hydraulic valve include electromagnetic drive, motor drive, and hydraulic drive. Electromagnetic drive has the characteristics of simple structure, high reliability, and low cost [7,8], and is the most common driving mode of the hydraulic valve [9].

The electromagnetic force of the switching electromagnet fluctuates greatly with the displacement in the working range. The mechanical vibration and impact noise generated by this electromagnet are large, and it is not easy to control the position [10]. An important difference between the proportional electromagnet and the ordinary electromagnet is that the electromagnetic force of the armature is not affected by its displacement and has an approximately horizontal displacement—electromagnetic force characteristic. The electromagnetic force is approximately constant in the working range of the armature, which is only related to the coil current. This phenomenon is called the constant force characteristic [11,12].

The proportional electromagnet is the basis for the continuous adjustment of the hydraulic valve. The output electromagnetic force by the electromagnet is controlled by changing the coil current, to continuously and proportionally control the movement of the valve core and use the reset spring to push the valve core back to its initial position. Xie et al. [13] used the FEM to simulate the proportional electromagnet for shock absorbers. By optimizing the parameters such as the basin mouth depth and the magnetic isolation ring inclination angle, the

constant force characteristics of the proportional electromagnet were improved, to continuously control the displacement of the proportional electromagnet valve core to adjust the pressure and flow of the hydraulic valve. Xu et al. [14] designed a proportional electromagnet for electromagnet-driven shock absorbers. They established an accurate model of a proportional electromagnet composed of a pilot valve and a safety valve. This model serves as a valuable tool for optimizing system design. Wei et al. [15] used a proportional electromagnet to drive the spool of a proportional pressure-regulating valve. The effects of orifice diameter, spring stiffness, and viscous damping coefficient on the stability and pressure of the spool were studied. The pressure was controlled by changing the coil current. Ledvon et al. [16] used a proportional electromagnet to drive the spool of the proportional directional valve and tested the static and dynamic characteristics of the proportional directional valve. Wang et al. [17] established two-dimensional and three-dimensional magnetostatic finite element analysis models of proportional electromagnets. They designed a static multi-objective optimization strategy based on a genetic algorithm to improve the static thrust of the actuator by optimizing the structural parameters of the actuator. Yuan et al. [18] designed a new type of proportional electromagnets for a pneumatic proportional directional valve and tested the displacement-electromagnetic force characteristics to ensure the unique automatic reset ability of the valve core. Yuan et al. [19] conducted a study on the pole shoe structure of a proportional solenoid actuator and conducted a detailed analysis of the impact of six different magnetic materials and geometric parameters on the constant force characteristics. Ercan et al. [20] designed and manufactured a proportional electromagnet for heavy vehicle braking system, analyzed the influence of key dimensional parameters on the force-displacement characteristics, and determined the optimal size. The static and dynamic characteristics of the electromagnet were studied theoretically and experimentally by Maxwell, but the displacement-force characteristic test curve of the electromagnet was not seen in the paper.

Through investigation, it is found that a proportional electromagnet with constant force characteristics is the basis for the excellent control performance of hydraulic valves. However, the constant force characteristics are related to many parameters, require special design, and are difficult to obtain. Many researchers have analyzed the factors that affect the constant force characteristics of proportional electromagnets but have not established a criterion for judging the constant force characteristics. In addition, the electromagnetic force is tested discretely, continuous testing curves of displacement-force and current-force characteristics of proportional solenoid valves are rare in previous literature. In this paper, the proportional electromagnet is designed under the condition of the minimum variance of the electromagnetic force under the rated current in the working range of the armature, the influence of the key structure on the constant force characteristics of the electromagnet is analyzed, and the constant force characteristics and output characteristics were continuously tested. The related research deepens the understanding of how the key parameters affect the constant force characteristics and helps designers to design these parameters to develop new structures, which have certain practical engineering value.

The rest of this paper is structured as follows. Section 2 introduces the structure and the working principle of the proportional electromagnet. The mechanism of the constant force characteristics of the proportional electromagnet is explained in detail and the mathematical model of the electromagnetic force is established. Section 3 mainly uses the FEM to analyze the influence of the key structure on the constant force characteristics of the electromagnet. In Section 4, the test bench of the electromagnet is built to test the constant force characteristics and output characteristics. Section 5 is the conclusion of this paper.

2. Structure and Working Principle of Proportional Electromagnets

2.1. Structure of Proportional Electromagnets

The electromagnet mainly comprises a coil, coil skeleton, electromagnet shell, electromagnet inner cylinder, magnetic isolation ring, armature, limit ring, pole shoe, and valve core. The structure diagram of the electromagnet is shown in Figure 1. The armature is outside the valve core and is integrated with an interference fit. The valve core slides with the inner wall of the electromagnet inner cylinder and the pole electromagnet inner cylinder, magnetic isolation ring, and pole interference fit. The electromagnet electromagnet inner cylinder, armature, and pole shoe use materials with magnetic conductivity. The magnetic isolation ring has the magnetic isolation ability and is installed between the electromagnet inner cylinder and the pole shoe. The limit ring is set outside the valve core and is located between the armature and the pole shoe to prevent the armature from being too close to the pole shoe, resulting in a surge of electromagnetic force on the armature. The green and red lines are wires.

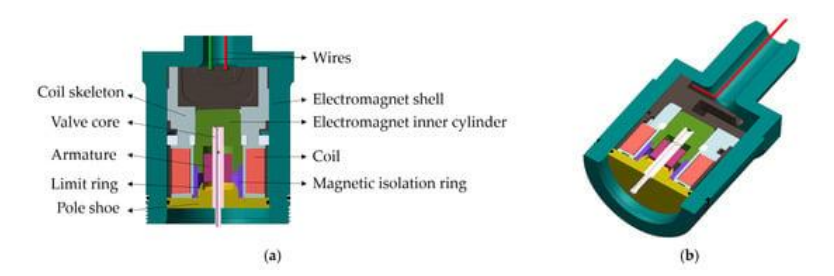


Figure 1: Structure diagram of electromagnet. (a) Electromagnet structure plane diagram. (b) Electromagnet structure stereogram.

2.2. Working Principle of Proportional Electromagnets

By controlling the coil current, the output electromagnetic force by the electromagnet overcomes the spring force to continuously and proportionally drive the valve core. The magnetic circuit diagram of the proportional electromagnet is shown in Figure 2, the green line represents armature displacement and the dotted line indicates the magnetic flux path. When the current is applied to the coil, the coil generates a magnetic potential and forms two circuits of ϕ_1 and ϕ_2 .

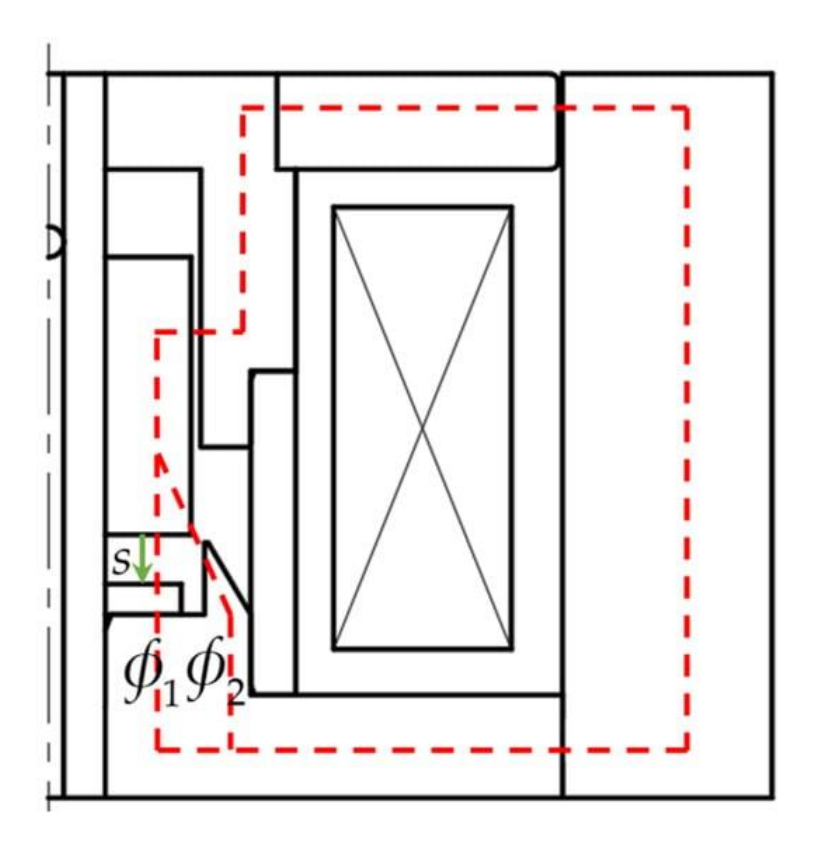


Figure 2: Magnetic circuit diagram of proportional electromagnets.

The magnetic circuit ϕ_1 penetrates the working atmosphere from the pole shoe basin bottom, enters the armature axially, and then passes through the electromagnet inner cylinder, the magnetic conduction channel in the coil skeleton and the electromagnet shell, and returns to the pole shoe to form a circuit. Because the magnetic isolation ring is made of copper with low permeability, the magnetic circuit ϕ_2 rarely enters the electromagnet inner cylinder through the magnetic isolation ring and merges with the magnetic circuit ϕ_1 to form a loop, and most of them enter the

armature through the inclination angle on the pole shoe and converge with the magnetic circuit ϕ_1 . Since the magnetic field line is always closed along the path with the smallest magnetoresistance and has the tendency to shorten the closed path, the armature has a downward trend due to the electromagnetic force. Because of the effect of magnetic circuit ϕ_1 , the pole shoe basin bottom produces an axial downward electromagnetic force F_{e1} to the armature. downward movement of the armature will reduce the magnetic resistance on the magnetic circuit ϕ_1 . The closer the armature is to the pole shoe basin bottom, the greater the axial electromagnetic force F_{e1} is. When the armature moves to the position where it fits with the pole shoe basin bottom, the axial electromagnetic force F_{el} rises sharply, which needs to be avoided in practical applications. Therefore, a limit ring is installed in the design to prevent the armature from moving to this position. Because of the magnetic circuit ϕ_2 , the inclination angle on the pole shoe generates an electromagnetic force $F_{\rm e2}$ with an axial component on the armature. When the armature is far away from the pole shoe basin bottom, the magnetic line of force mainly passes through the magnetic circuit ϕ_2 , and the electromagnetic force $F_{\rm e2}$ has an increasing trend when the armature is close to the pole shoe basin bottom. When the armature is close to the pole shoe basin bottom, the magnetic circuit ϕ_1 has a shunt effect on the magnetic circuit ϕ_2 , and the electromagnetic force $F_{\rm e2}$ will decrease. In addition, the armature is close to the pole shoe basin bottom, which makes the angle between the electromagnetic force F_{e2} and the axial direction too large and reduces the axial component of the electromagnetic force F_{e2} . Through the superposition of these two electromagnetic forces, the total electromagnetic force $F_{\rm e}$ of the armature is formed. In the working range of the armature, the electromagnetic force F_e is not affected by the change in the displacement of the armature s, and remains constant, as shown in Figure 3.

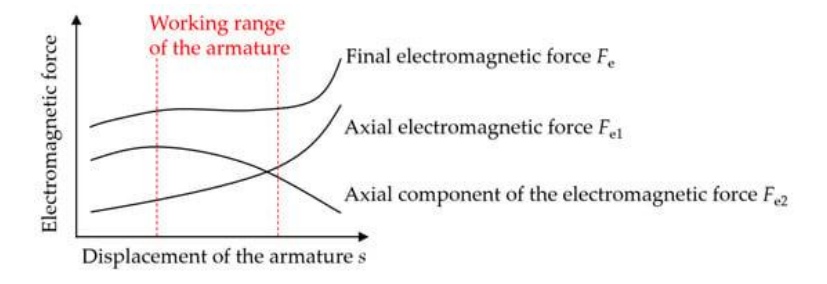


Figure 3: Electromagnetic force of proportional electromagnets.

2.3. Mathematical Model of Electromagnetic Force

There are usually three methods for calculating electromagnetic force, namely the empirical equation method, magnetic circuit segmentation method, and finite element method (FEM). The following will use the magnetic circuit segmentation method to analyze the electromagnetic force.

The coil can be simplified as a series structure of resistance R and inductance L, and the equivalent circuit is shown in Figure 4.

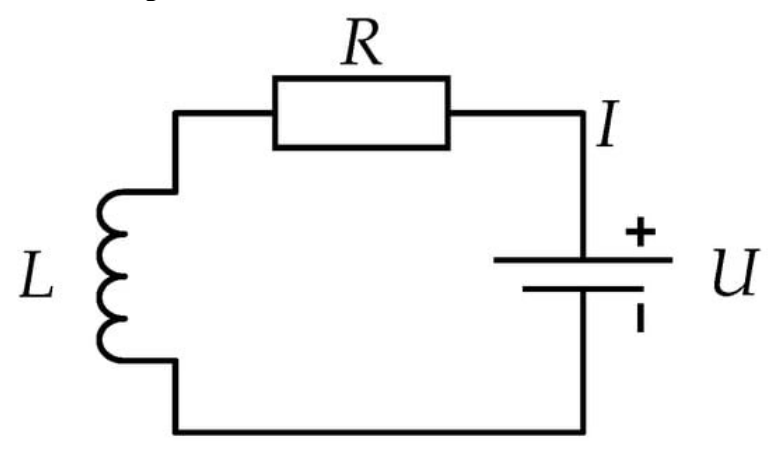


Figure 4: The equivalent circuit of the coil.

According to Kirchhoff's voltage law, the circuit model of the coil can be expressed by Equation (1):

$$u = IR + \frac{d\varphi}{dt} = IR + L\frac{dI}{dt} \tag{1}$$

where U is the coil voltage, φ is the main magnetic flux linkage, I is the coil current, R is the coil resistance, L is the coil inductance, and t is time.

The magnetic circuit can be compared with the circuit. To maintain a certain magnetic flux in the magnetic circuit, there must be a certain magnetomotive force. The magnitude of the magnetomotive force is equal to the product of the current and the number of turns, that is, the number of ampere-turns. According to the magnetic circuit Ohm's law, the equation can be obtained:

$$\emptyset = N \cdot I / \sum R_e \tag{2}$$

where ϕ is the magnetic flux, N is the number of turns of the coil, and $\Sigma R_{\rm e}$ is the total reluctance of the magnetic circuit. In the calculation of magnetoresistance, the magnetic circuit segmentation method is usually used to analyze the magnetic circuit of the electromagnet. The magnetic circuit analysis diagram of the electromagnet is shown in Figure 5, and the structural parameters of the electromagnet are shown in Figure 6.

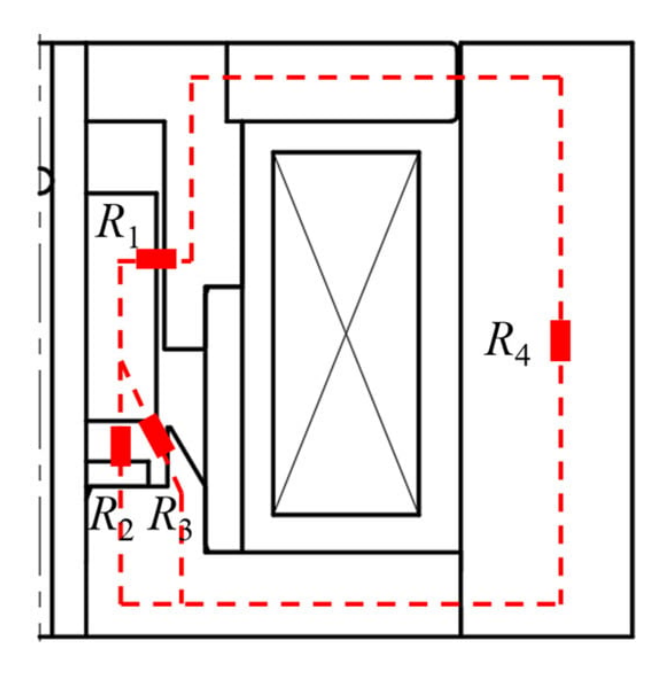


Figure 5: Magnetic circuit analysis diagram of electromagnet.

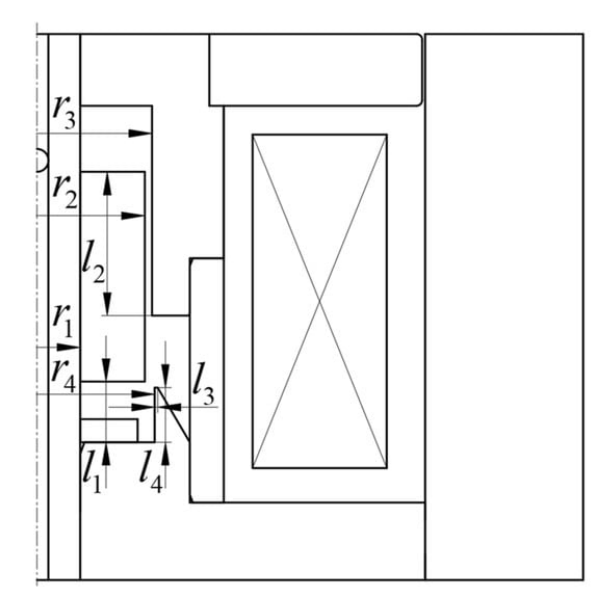


Figure 6: Structural parameters of electromagnet.

Each magnetoresistance after magnetic circuit separation is calculated by the calculation equation of magnetoresistance, and then the total reluctance of the magnetic circuit is calculated according to the series and parallel relationship of reluctance shown in Figure 5. The general equation of magnetoresistance is [21,22]:

$$R_e = \frac{L_e}{\mu S_e} \tag{3}$$

where $R_{\rm e}$ is the magnetoresistance, $L_{\rm e}$ is the length of the medium, $S_{\rm e}$ is the cross-sectional area of the medium, and μ is the permeability of the medium.

Magnetoresistance R_1 is the reluctance generated by the non-working air gap between the armature and electromagnet inner cylinder. As shown in Figure 5, the air gap is filled with oil and can be expressed by Equation (4):

$$R_1 = \frac{r_3 - r_2}{\mu_0 \cdot \pi (r_2 + r_3) \cdot (l_2 - s)} \tag{4}$$

where r_2 is the radius of the armature, r_3 is the inner radius of the electromagnet inner cylinder, l_2 is the air gap length between the armature and electromagnet inner cylinder, and μ_0 is the oil permeability.

Magnetoresistance R_2 is the reluctance generated by the working air gap between the pole shoe basin bottom and the front surface of the armature. As shown in Figure 5, the air gap is filled with oil and can be expressed by Equation (5):

$$R_2 = \frac{l_1 - s}{\mu_0 \pi (r_2^2 - r_1^2)} \tag{5}$$

where l_1 is the maximum length of the front surface of the armature from the pole shoe basin bottom, and r_1 is the radius of the valve core.

Magnetoresistance R_3 is an irregular magnetoresistance generated by the air gap between the armature and the inclination

angle on the pole shoe. With the displacement of the armature, it is difficult to express the reluctance with an accurate mathematical equation.

Magnetoresistance R_4 is the total magnetic resistance of magnetic conductive materials such as pole shoe, armature, electromagnet inner cylinder, part of coil skeleton, and electromagnet shell. Due to the tight connection between the various parts, the magnetic flux leakage phenomenon is small, and the permeability of the magnetic material is larger than that of the oil, so the value of R_4 can be ignored.

After obtaining the reluctance of each part in the magnetic circuit, according to the series and parallel relationship of the reluctance shown in Figure 5, the total reluctance of the magnetic circuit can be calculated as Equation (6):

$$\sum R_e = R_1 + \frac{R_2 \cdot R_3}{R_2 + R_3} + R_4 \tag{6}$$

Assuming that the magnetic energy stored in the electromagnet is used to drive the movement of the armature, the expression of the electromagnetic force on the armature is:

$$F_e = \frac{\emptyset^2}{2\mu_0 S} = \frac{\emptyset^2}{2\mu_0 \pi (r_2^2 - r_1^2)} \tag{7}$$

where *S* is the magnetic flux cross-sectional area of the working air gap.

According to Equation (7), the magnitude of the electromagnetic force is proportional to the square of the magnetic flux. To keep the electromagnetic force of the armature from being affected by the displacement of the armature, it is necessary to keep the total magnetoresistance of the electromagnet constant during the of the armature. calculation movement The of magnetoresistance R_1 and R_2 is relatively easv. magnetoresistance R_3 , the calculation is very complicated, and there is no mature calculation theory at present. Therefore, this paper uses the FEM to analyze in Section 3.

3. Parametric Analysis of Key Parameters of Electromagnet

The FEM discretizes and solves each component in the solution area of the electromagnet. The obtained electromagnetic force result is more accurate than the other two calculation methods, which is an effective means to study the electromagnetic force [3]. Using the FEM, the results of magnetic flux cloud and electromagnetic force can be obtained, and the influence of different structures on the electromagnetic force—displacement curve can be quickly analyzed by parameterization [23-25]. Maxwell 19.4 software is practical electromagnetic force analysis software. Based on Maxwell's differential equation and finite element discrete method, the results of magnetic flux cloud diagram and electromagnetic force can be obtained, and the influence of different structures on the electromagnetic force—displacement curve can be quickly analyzed by parameterization.

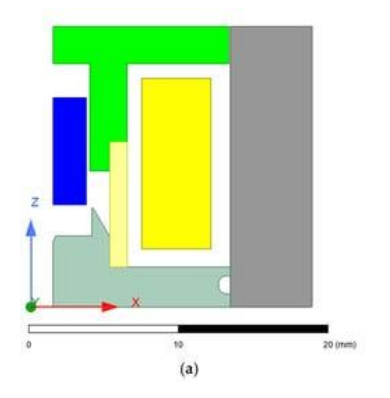
3.1. Simulation Settings

(1) Solver type

Because the purpose of this simulation is to solve the static electromagnetic force, the static magnetic field solver is used to analyze the electromagnet. Because the electromagnet is an axisymmetric structure, to shorten the calculation time, the Maxwell 2D module is used for simulation research.

(2) Model

From Figure 1, the electromagnet designed in this paper is an axisymmetric structure. To improve the simulation efficiency, reduce the calculation workload, and save the simulation time, the axisymmetric model is established to solve the problem. Ignoring the non-metallic materials in the electromagnet, merging and simplifying some parts with the same function [26], the simulation model of the electromagnet with z as the axis is established as shown in Figure 7.



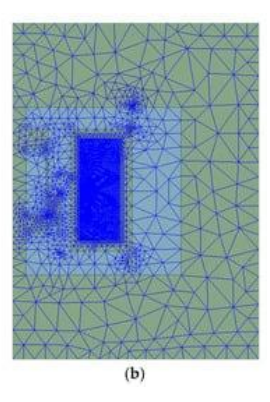


Figure 7: Electromagnet finite element simulation model and meshing. (a) Electromagnet finite element simulation model. (b) Electromagnet meshing.

The material selection of each part of the electromagnet is shown in Table 1.

Table 1: Material selection table for each part of the electromagnet.

Part	Material
Electromagnet shell	1215 steel
Pole shoe	1215 steel
Electromagnet inner cylinder	1215 steel
Part of the coil skeleton	1215 steel
Armature	1215 steel
Magnetic isolation ring	Copper
Coil	Copper

1215 steel is a magnetic material, and copper is a material with low permeability.

(3) Boundary

The static magnetic field solver contains a variety of boundary conditions, among which the balloon boundary condition is the most commonly used one. The balloon boundary avoids a large solution area and reduces the calculation workload, so it is determined that the balloon boundary condition is used in this model.

(4) Excitation

In the static magnetic field solver, the excitation is selected as the current source, that is, the number of ampere-turns. The number of turns of the drive coil used is 420, the resistance of the coil is 4.7Ω , and the current of the input coil is up to 2.0 A.

(5) Mesh division

When the static magnetic field solver is solved, it has the function of adaptive mesh generation. If the mesh generation of the model is not fine enough, the calculation results are not convergent. The system will automatically encrypt the mesh of the key areas to obtain a better mesh generation effect. Electromagnet meshing is shown in Figure 7.

(6) Parameters

The solution parameter is set as the electromagnetic force of the electromagnet, which is defined as Force, and the motion type of the electromagnet is Move.

3.2. Parametric Simulation of Proportional Electromagnets

By analyzing the working principle of the proportional electromagnet, the shape of the pole shoe can change the direction of the magnetic circuit in the air gap. The design of the pole shoe is a key part of the magnetic circuit design of the electromagnet, and it is the key to whether the electromagnet has constant force characteristics.

The following content will take the constant force characteristics of the electromagnet as the goal. The sensitivity analysis of the key parameters affecting the constant force characteristics of the electromagnet on the pole shoe, namely the basin bottom radius r_4 , the guide angle width l_3 , and the basin mouth depth l_4 will be carried out. The initial values of the structural parameters of the electromagnet are shown in Table 2.

Parameter	Parameter Value/mm
Valve core radius r_1	1.50
The radius of the armature r_2	3.25
The internal radius of electromagnet inner cylinder r_3	4.00
Basin bottom radius r_4	4.10
The maximum length of the front surface of the armature from the pole shoe basin bottom l_1	2.10
The air gap length between the armature and electromagnet inner cylinder l_2	5.00
Guide angle width l_3	0.10
Basin mouth depth l ₄	1.90

Table 2: Initial values of the structural parameters of the electromagnet.

To fully understand the electromagnetic force of the armature at different positions, the simulation range of the armature is set to 2.0 mm, that is, the front surface of the armature is 0.1 mm nearest to the pole shoe basin bottom. The parameterization analysis of each parameter is carried out under the working condition of 2.0 A, and the structural parameters that give the electromagnet constant force characteristics are determined. Because the electromagnetic force is not constant in the working range, there will be small fluctuations. To accurately study the constant force characteristics, this paper will use the variance of the electromagnetic force of the armature in the working range as a quantitative index to evaluate the constant force characteristics. The calculation equation of electromagnetic force variance is:

$$S^{2} = \frac{1}{n} \sum_{i=1}^{n} (F_{ei} - \overline{F}_{e})^{2}$$
 (8)

The variance reflects the degree of data fluctuation. In the working range of the armature, the smaller the variance of the electromagnetic force, the smaller the influence of the displacement of the armature on the electromagnetic force of the armature, that is, the closer the electromagnet is to the constant force characteristic.

(1) The influence of basin bottom radius r_4

Keeping l_3 and l_4 unchanged as the initial values, r_4 is selected as 3.8 mm, 3.9 mm, 4.0 mm, 4.1 mm, and 4.2 mm respectively to

simulate the electromagnetic force of the armature. The influence of r_4 on the electromagnetic force of the armature is shown in Figure 8, and the influence of r_4 on the variance of the electromagnetic force in the working range is calculated as shown in Figure 9.

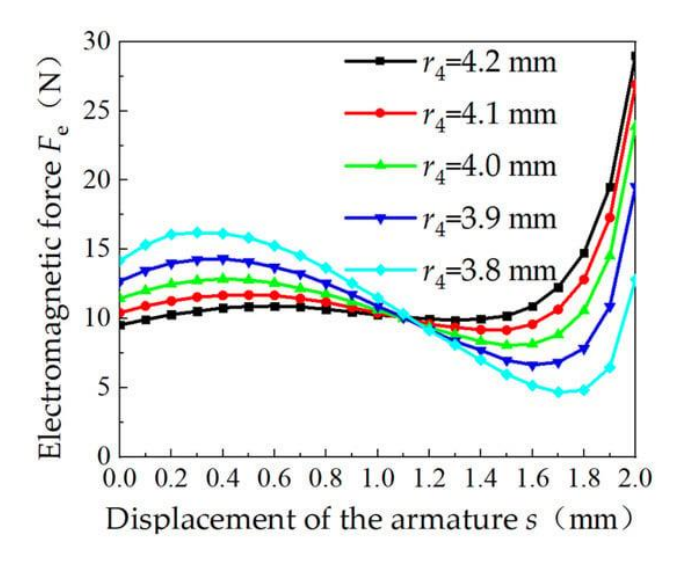


Figure 8: Influence of r_4 on electromagnetic force.

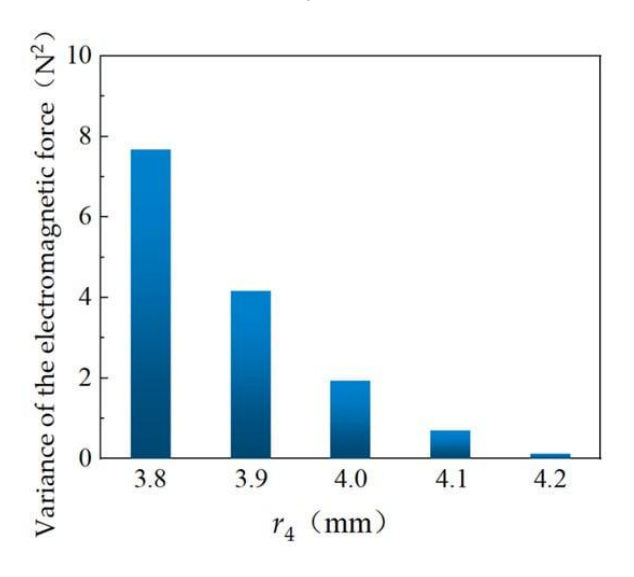


Figure 9: Influence of r_4 on the variance of electromagnetic force.

It can be seen from Figure 8 that the influence of r_4 on the electromagnetic force of the armature is obvious. The larger the r_4 , the smaller the fluctuation of the electromagnetic force of the armature, that is, the smaller the influence of the displacement of the armature on the electromagnetic force of the armature. With the increase in the displacement of the armature, the electromagnetic force of the armature increases first, then decreases, and then increases. When the displacement of the armature is small, the electromagnetic force of the armature is greatly affected by the electromagnetic force F_{e2} . When the displacement of the armature increases to a certain value, the electromagnetic force of the armature is greatly affected by the electromagnetic force F_{el} . The electromagnetic force F_{e} of the armature is the result of the superposition of the electromagnetic force F_{e1} and the electromagnetic force F_{e2} . Through the observation of Figure 8, the armature displacement of 0.3~1.3 mm is selected as the working range of the armature.

From Figure 9, r_4 has an obvious influence on the variance of the electromagnetic force on the armature. In the working range, the larger the r_4 , the smaller the variance of the electromagnetic force on the armature. The selection of r_4 is based on the minimum variance of the electromagnetic force received by the armature in the working range. When r_4 is 4.2 mm, the variance of the electromagnetic force received by the armature is 0.13 N^2 .

(2) The influence of guide angle width l₃

Keeping l_4 unchanged as the initial values, r_4 is 4.2 mm, and l_3 is selected as 0.05 mm, 0.1 mm, 0.6 mm, and 1.1 mm respectively to simulate the electromagnetic force of armature. The influence of l_3 on the electromagnetic force is shown in Figure 10, and the influence of l_3 on the variance of electromagnetic force in the working range is shown in Figure 11.

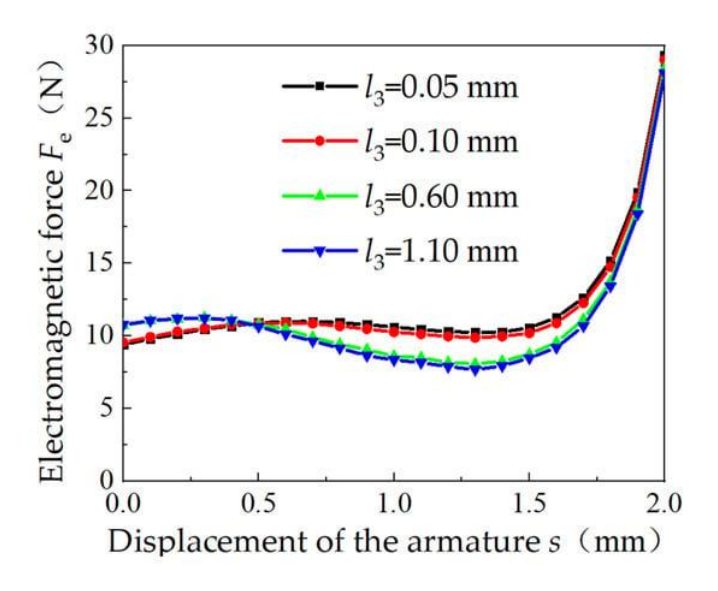


Figure 10: Influence of l_3 on electromagnetic force.

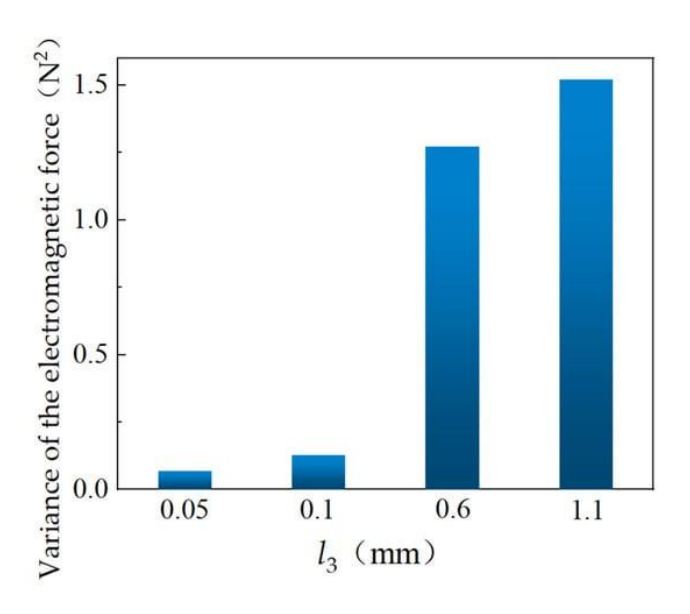


Figure 11: Influence of l_3 on the variance of electromagnetic force.

It can be seen from Figure 10 that the influence of l_3 on the electromagnetic force of the armature is obvious. In the working

range, the smaller the l_3 , the smaller the fluctuation of the electromagnetic force of the armature, that is, the smaller the influence of the displacement of the armature on the electromagnetic force of the armature.

It can be seen from Figure 11 that in the process of l_3 changing from 0.1 mm to 0.6 mm, the variance of the electromagnetic force of the armature changes greatly, and the changes from 0.05 mm to 0.1 mm and from 0.6 mm to 1.1 mm are relatively small. In the working range, the smaller the l_3 , the smaller the variance of the electromagnetic force on the armature. The selection of l_3 is based on the minimum variance of the electromagnetic force in the working range. Although the variance of the electromagnetic force received by the armature is the smallest when l_3 is 0.05 mm, considering the processing difficulty of the pole shoe and the durability of the electromagnet, and when l_3 is 0.05 mm and 0.1 mm respectively, the variance of the electromagnetic force received by the armature is not much different, so l_3 is selected as 0.1 mm.

(3) The influence of basin mouth depth l_4

Keeping r_4 is 4.2 mm, l_3 is 0.1 mm, and l_4 is selected as 1.7 mm, 1.8 mm, 1.9 mm, 2.0 mm, and 2.1 mm respectively to simulate the electromagnetic force of armature. The influence of l_4 on the electromagnetic force of the armature is shown in Figure 12, and the influence of l_4 on the variance of the electromagnetic force in the working range is shown in Figure 13.

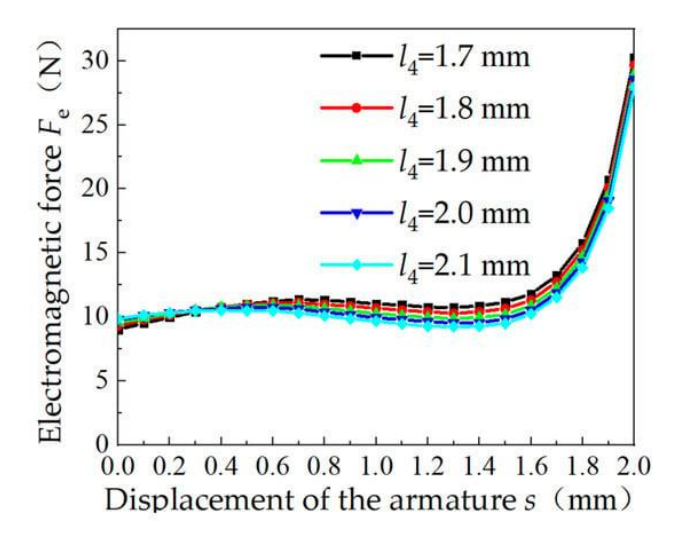


Figure 12: Influence of l_4 on electromagnetic force.

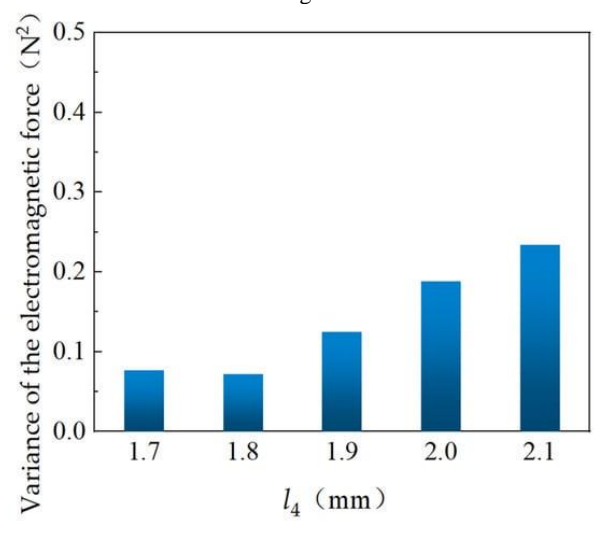


Figure 13: Influence of *l*⁴ on the variance of electromagnetic force.

It can be seen from Figure 12 that the influence of l_4 on the electromagnetic force of the armature is limited. In the working range, the smaller the l_4 , the smaller the fluctuation of the electromagnetic force of the armature. Figure 13 shows that l_4 has little effect on the variance of the electromagnetic force on the armature. In the working range, the variance of the

electromagnetic force on the armature is the smallest when l_4 is 1.8 mm. The selection of l_4 is based on the minimum variance of the electromagnetic force received by the armature in the working range, so l_4 is selected as 1.8 mm.

After the sensitivity analysis of r_4 , l_3 , and l_4 , the values that give the electromagnet constant force characteristics are determined. r_4 is selected as 4.2 mm, l_3 is selected as 0.1 mm, l_4 is selected as 1.8 mm.

3.3. Electromagnetic Force Simulation

Based on the key parameters of the electromagnet determined above, the coil current is set to be 0.5 A, 1.0 A, 1.5 A, and 2.0 A, respectively, and the armature is in the initial position (s = 0 mm). The distribution of the magnetic field line and the magnetic induction intensity of the electromagnet are simulated. The distribution of the magnetic field line and the magnetic induction intensity at different input currents are obtained as shown in Figure 14.

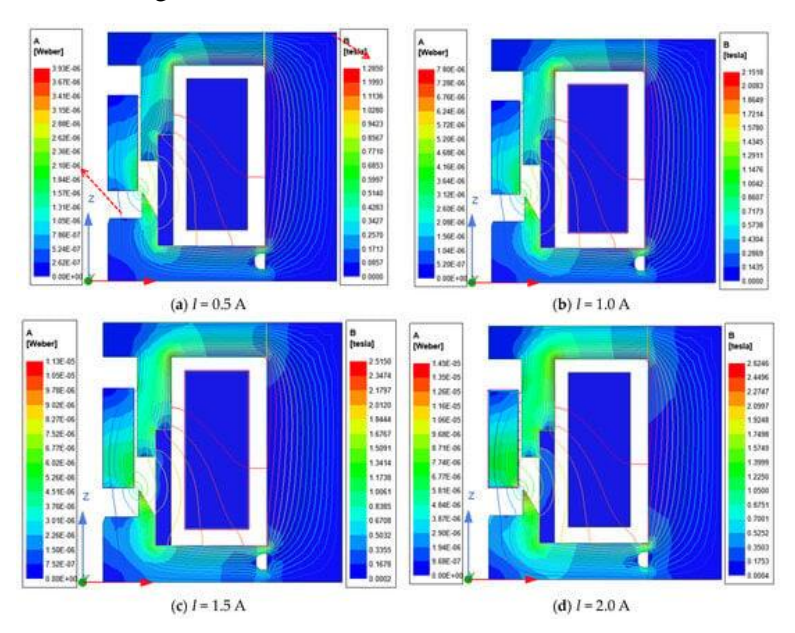


Figure 14: The distribution of magnetic field lines and magnetic induction intensity when different currents are input. (A stands for magnetic flux and B stands for magnetic induction).

It can be seen from Figure 14 that the closer to the coil and the larger the input current is, the denser the distribution of the magnetic lines is and the greater the magnetic induction in intensity is. The distribution of magnetic field lines on the electromagnet inner cylinder, armature, and pole shoe is denser than that of the electromagnet shell, and the magnetic induction intensity is also significantly larger than that of the electromagnet shell, which is caused by the larger cross-sectional area of the electromagnet shell.

To more intuitively observe the distribution of magnetic lines of force and magnetic induction intensity of the armature at different positions when the proportional electromagnet is working, the proportional electromagnet of the armature at different positions is simulated and analyzed below. When the input current is 2.0 A, the distribution of magnetic lines of force and magnetic induction intensity of the armature at different positions is shown in Figure 15.

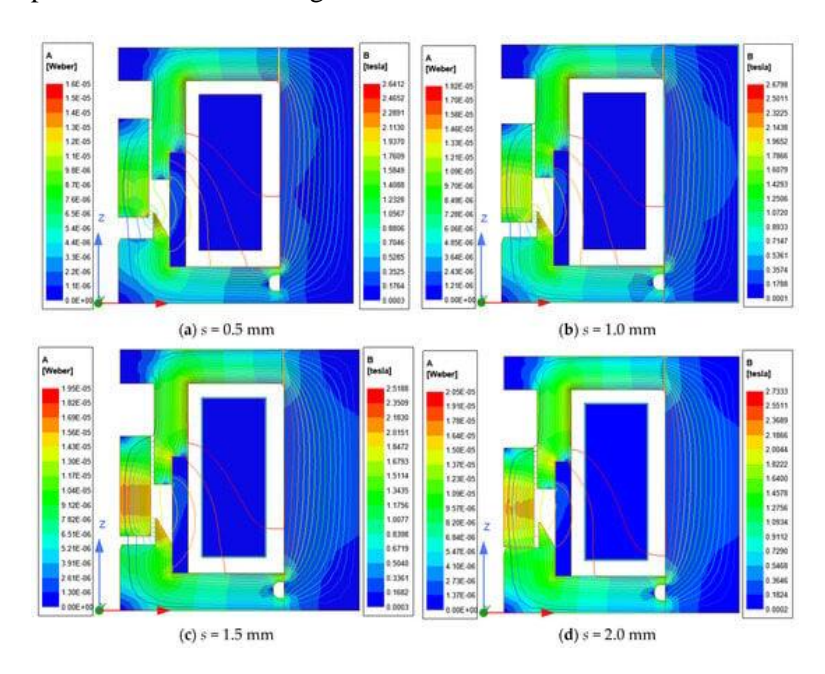


Figure 15: Distribution of magnetic field line and magnetic induction intensity of armature at different positions.

Figure 15 again verifies the correctness of the above analysis of the working principle of the proportional electromagnet.

When the armature is far away from the pole shoe basin bottom, the magnetic line of force mainly passes through the magnetic circuit ϕ_2 , the electromagnetic force F_{e2} is larger, and the electromagnetic force F_{el} is smaller. The downward movement of the armature reduces the magnetic resistance on the magnetic circuit ϕ_1 , and the electromagnetic force F_{e1} becomes larger. When the armature moves to the position where it will fit the pole shoe basin bottom, the axial electromagnetic force F_{e1} rises the armature moves downward, When electromagnetic force $F_{\rm e2}$ increases. When the armature is close to the pole shoe basin bottom, the magnetic circuit ϕ_1 plays a diversion role in the magnetic circuit ϕ_2 , and the electromagnetic force F_{e2} will decrease. In addition, the armature is close to the pole shoe basin bottom, and the angle between electromagnetic force F_{e2} and the axial direction is too large, which also reduces the axial component of the electromagnetic force F_{e2} . superposition Through the of these electromagnetic forces, the total electromagnetic force F_e of the armature is formed. In the working range of the armature, the electromagnetic force F_e is not affected by the change in the displacement s of the electromagnet and remains constant.

The coil current is set to 0.5 A, 1.0 A, 1.5 A, and 2.0 A respectively. The electromagnetic force of the armature is simulated, and the simulation results of the displacement–force characteristics of the electromagnet are obtained, as shown in Figure 16.

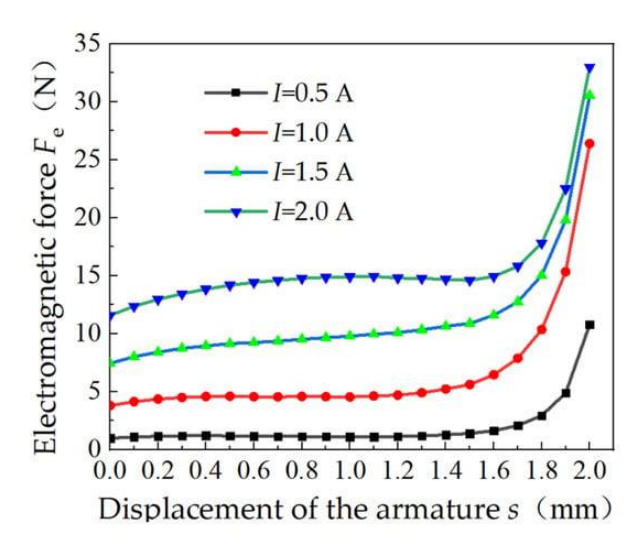


Figure 16: Displacement–force characteristic simulation curve of electromagnet.

From Figure 16, the electromagnet has perfect constant force characteristics in the working range of the armature displacement of 0.3~1.3 mm. In the working range of the armature, the displacement of the armature is 0.8 mm, and the coil current is set as a slope signal from 0 A to 2.0 A. The current–force characteristics of the electromagnet are simulated, and the simulation curve of the current–force characteristics of the electromagnet is obtained. The electromagnetic force of the armature under different currents is fitted, and the fitting curve of the current–force characteristics of the electromagnet is obtained, as shown in Figure 17.

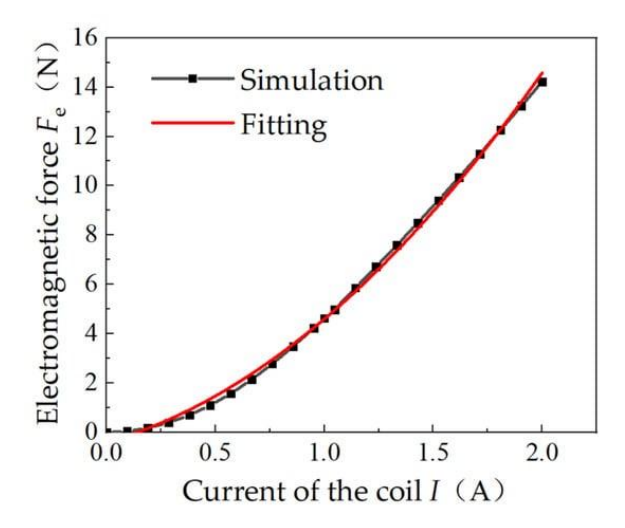


Figure 17: The current–force characteristic curve of electromagnet.

From Figure 17, the fitting curve of the current–force characteristics of the electromagnet is highly consistent with the simulation curve, and the R^2 is 0.998, which has met the actual needs in engineering applications. The fitting expression of the current–force characteristics of the electromagnet is obtained:

$$F_e = 2.5I + 2.5I^2 (9)$$

4. Test Verification of Proportional Electromagnets

4.1. Test Equipment

The electromagnetic force test bench is mainly composed of a displacement sensor, force sensor, servo motor, power supply, displacement controller, signal generator, fixture, and other components. As shown in Figure 18, the displacement–force characteristic curve and current–force characteristic curve of the electromagnet can be tested respectively.

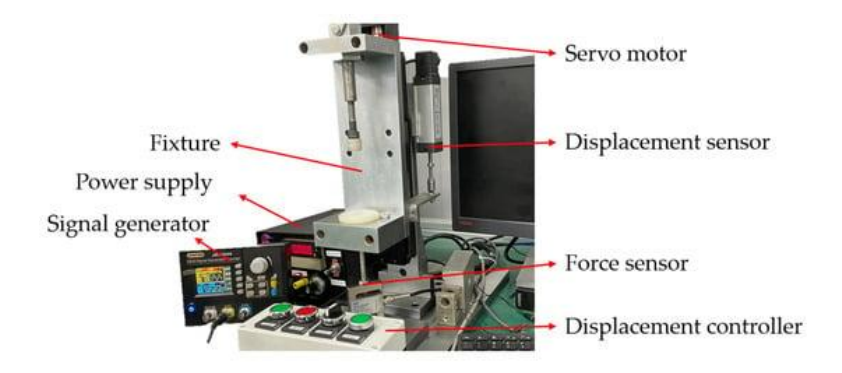


Figure 18: Electromagnetic force test bench.

The electromagnet is fixed on the electromagnetic force test bench by the fixture and is driven by a servo motor to move in the vertical direction. The displacement controller controls the position of the fixture and the electromagnet, which can test the electromagnetic force when the armature is in different positions and obtain the displacement—force characteristics of the electromagnet. The signal generator can output signals of various waveforms, provide various types of current for the coil, and obtain the current—force characteristics of the electromagnet.

4.2. Test Scheme

(1) Displacement–force characteristic test

In the displacement–force characteristic test of the electromagnet, the current of the coil is set to 0.4 A, 0.6 A, 0.8 A, 1.0 A, 1.2 A, 1.4 A, 1.6 A, 1.8 A, 2.0 A respectively. The displacement of the armature increases in the working range, and the electromagnetic force is tested.

(2) Current–force characteristic test

Taking the displacement of the armature at 0.8 mm, the current of the coil is set to the triangular waveform shown in Figure 19, and the electromagnetic force of the armature is tested.

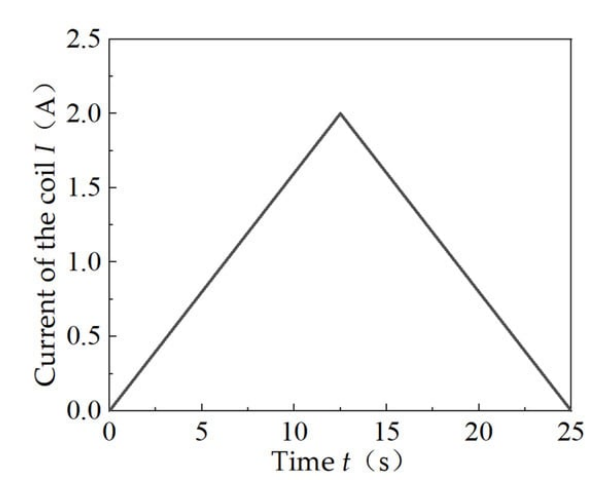


Figure 19: Current waveform of the coil.

4.3. Test Results

By testing the electromagnetic force of the armature, the displacement–force characteristic curve of the electromagnet is shown in Figure 20, and the variance of electromagnetic force under different currents is shown in Figure 21.

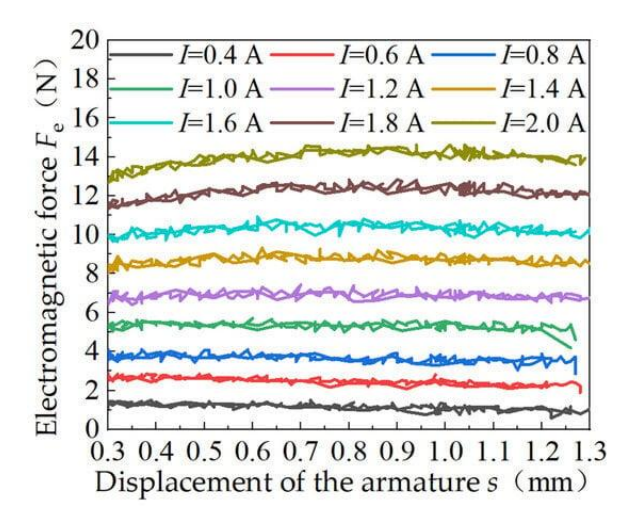


Figure 20: Displacement–force characteristic test curve of electromagnet.

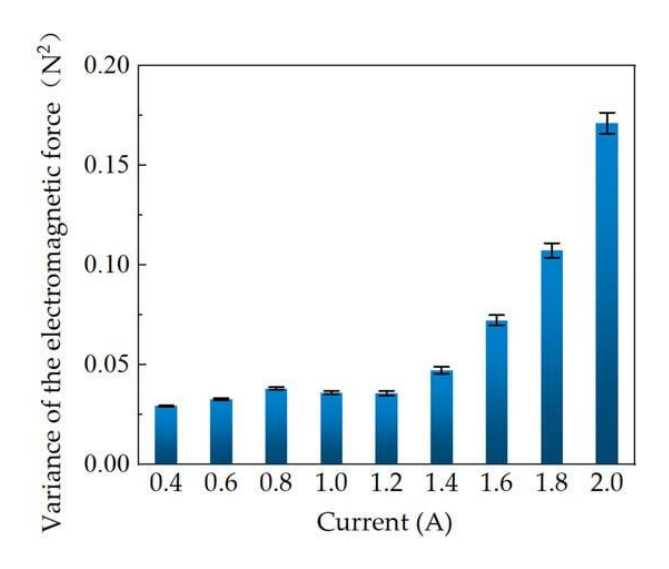


Figure 21: The variance of electromagnetic force under different currents.

Figure 20 shows that in the armature's working range, the electromagnetic force is maintained at a level that is not affected by the armature's displacement. Figure 21 shows that the variance of electromagnetic force under different currents is less than 0.2 N², its uncertainty is less than 0.005 N², and the electromagnet has constant force characteristics. The experimental results show that the proportional electromagnet studied in this paper has better constant force characteristics than previous studies.

Figure 22 shows the curve of the average electromagnetic force under different currents in the displacement–force characteristic test, and the red symbol is the error stick. The uncertainty of electromagnetic force is the largest when the current is 2 A, which is 0.4 N.

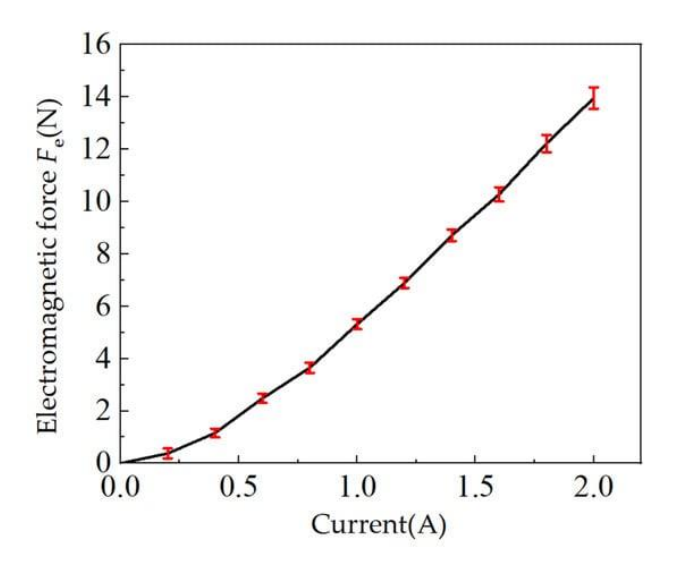


Figure 22: The curve of the average electromagnetic force under different currents.

Figure 23 shows the continuous test and simulation comparison curve of the electromagnet's current–force characteristic curve.

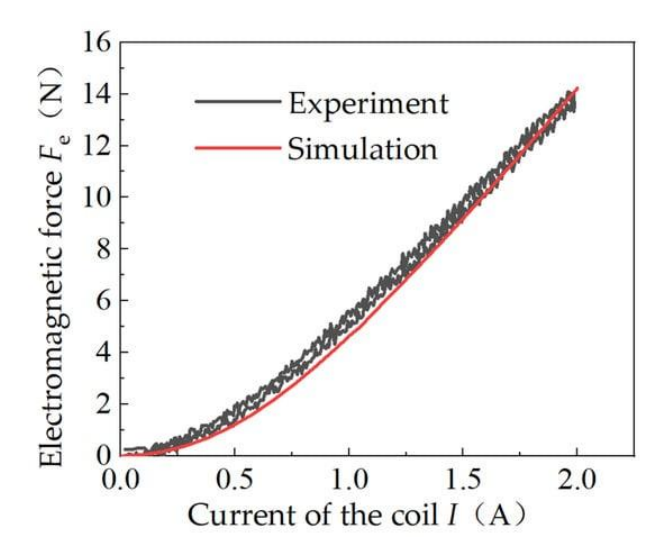


Figure 23: Current-force characteristic test and simulation comparison curve of electromagnet.

Figure 23 shows that the electromagnetic force increases with the increase in the coil current input, and the test results are highly consistent with the simulation results. The test results for the electromagnet's displacement–force characteristic agree with the simulation results. Through experimental comparison, the current–force characteristic simulation and test results of the proportional electromagnet obtained in this paper are more accurate than previous research.

5. Conclusions

In this paper, the influence of the key structure on the constant force characteristics of the electromagnet is analyzed. A proportional electromagnet for driving hydraulic valves is designed with the condition of the minimum variance of the armature's electromagnetic force in the armature's working range. The mechanism of the constant force characteristics of the proportional electromagnet is explained in detail, the mathematical model of the electromagnetic force is established, and the electromagnet is simulated and analyzed. The following conclusions are obtained:

(1) The influences of the basin bottom radius, the guide angle width, and the basin mouth depth on the constant force characteristics of the electromagnet were studied by the FEM. The influence of the basin bottom radius on the electromagnetic force of the armature is obvious. In the working range of the armature displacement, the larger the basin bottom radius, the smaller the influence of the armature displacement on the electromagnetic force of the armature. The influence of the guide angle width on the electromagnetic force of the armature is also obvious. In the working range of the armature displacement, the smaller the guide angle width, the smaller the influence of the armature displacement on the electromagnetic force of the armature. The basin mouth depth has a limited influence on the electromagnetic force of the armature. In the working range of the armature displacement, the smaller the basin mouth depth is, the smaller the fluctuation of the electromagnetic force of the armature is. Their values are found respectively to give the electromagnet constant force characteristics. When the basin bottom radius, the guide angle width, and the basin mouth depth

- are 4.2 mm, 0.1 mm, and 1.8 mm respectively, the electromagnet has better constant force characteristics.
- (2) The FEM simulation analysis of the designed electromagnet is carried out, and the displacement–force characteristics and current–force characteristics simulation curves of the electromagnet are obtained. The current–force characteristics of the electromagnet are fitted, and the fitting curve is highly consistent with the simulation curve. The fitting expression is $F_e = 2.5I + 2.5I^2$, and R^2 is 0.998, which can meet the actual needs of engineering applications.
- (3) The test bench of the electromagnet is built to test its constant force characteristics and output characteristics. The continuous displacement—force and current—force characteristics of the proportional electromagnet were tested. The test results of the displacement—force characteristics of the electromagnet show that the electromagnetic force is not affected by the displacement of the armature in the working range, and the designed electromagnet has perfect constant force characteristics. The test results of the current—force characteristics of the electromagnet are highly consistent with the simulation results, which will lay a foundation for the continuous control of the hydraulic valve. The related research deepens the understanding of how the key parameters affect the constant force characteristics and helps designers optimize these parameters to develop new structures with certain practical engineering values.

References

- Xu B, Shen J, Liu S, Su Q, Zhang JH. Research and Development of Electro-hydraulic Control Valves Oriented to Industry 4.0: A Review. Chin. J. Mech. Eng. 2020; 33: 552–559.
- 2. Wang H, Chen Z, Huang JH, Quan L, Zhao B. Development of High-Speed On-Off Valves and Their Applications. Chin. J. Mech. Eng. 2022; 35: 37–57.
- 3. Zhao JG, Luo L, Zhuo Y, Wang MH, He C, et al. Mechanical Characteristics and Miniaturization Design of the Electromagnetic Valve Used in Drilling Robots. Processes. 2024; 12: 16-85.

- 4. Pîslaru-Dănescu L, Morega AM, Morega M, Dobre AA. Prototyping a Proportionally Electromagnetic Actuator with Wide Displacement of its Mobile Part. In Proceedings of the 2019 11th International Symposium on Advanced Topics in Electrical Engineering (ATEE), Bucharest, Romania, 28–30 March 2019; 1–7.
- 5. Davide C, Andrea V. The Modeling of Electrohydraulic Proportional Valves. J. Dyn. Syst. Meas. Control. 2011; 134: 021008.
- 6. Lankin MV, Lozin OI, Lankina MY. Magnetization Dynamic Characteristics Models for Hydraulic Drives of Proportional Electromagnets. Procedia Eng. 2017; 206: 443–448.
- 7. Wang SJ, Weng ZD, Jin B, Cai HX. Multi-objective genetic algorithm optimization of linear proportional solenoid actuator. J. Braz. Soc. Mech. Sci. Eng. 2021; 43: 2.
- 8. Yue DL, Li LF, Wei LJ, Liu ZG, Liu C, et al. Effects of Pulse Voltage Duration on Open-Close Dynamic Characteristics of Solenoid Screw-In Cartridge Valves. Processes. 2021; 9: 17-22.
- 9. Li YC, Li RC, Yang JR, Yu XD, Xu JK. Review of Recent Advances in the Drive Method of Hydraulic Control Valve. Processes. 2023; 11: 2537.
- Wang SH, Xiao XL, Xiong GY. Direct Current Electromagnets with Constant Traction Characteristic. Chin. J. Mech. Eng. 2008; 44: 244–247.
- 11. Shang RK, Liu P, Quan WW, Ouyang YW. Comparative Analysis of Armature Structure on Constant Force Characteristics in Long-Stroke Moving-Iron Proportional Solenoid Actuator. Actuators. 2024; 13: 408.
- 12. Xue L, Fan X, Tao GL. Development of test system for proportional electromagnet actuators' performance. Mech. Electr. Eng. Mag. 2009; 26: 67–69.
- 13. Xie FW, Zhou R, Wang DS, Ke J, Guo XJ, et al. Simulation Study on Static and Dynamic Characteristics of Electromagnet for Electro-Hydraulic Proportional Valve Used in Shock Absorber. IEEE Access. 2020; 8: 41870–41881.
- 14. Xu JN, Kou F, Zhang XQ, Wan GH. Modeling and testing for continuously adjustable damping shock absorber equipped with proportional solenoid valve. J. Mech. Sci.

- Technol. 2023; 37: 3851-3866.
- 15. Wu W, Wei CH, Zhou JJ, Hu JB, Yuan SH. Numerical and experimental nonlinear dynamics of a proportional pressure-regulating valve. Nonlinear Dyn. 2021; 103: 1415–1425.
- Marian L, Lumír H, Adam B, Martin V. Static and dynamic characteristics of proportional directional valve. EPJ Web. Conf. 2019; 213: 02052.
- 17. Wang S, Weng Z, Jin B. A performance improvement strategy for solenoid electromagnetic actuator in servo proportional valve. Appl. Sci. 2020; 10: 4352.
- 18. Yue FY, Guo LT, Hao L, Wei B. Study of a Bidirectional Proportional Electromagnet. Appl. Mech. Mater. 2013; 2218: 155–158.
- 19. Yuan XJ, Ling HT, Qiu TY, Zhou JW, Zhao R. Optimization for a proportional electro-magnet with high accuracy utilizing finite element method. Int. J. Appl. Electromagn. Mech. 2021; 65: 267–280.
- 20. Ercan D, Gürsel Ş. Design and Analysis of a Proportional Electromagnet with Experimental Validation for Static and Dynamic Behavior. Preprints. 2024; 2024101770.
- 21. Yang L, Gao TX, Du XM, Zhai FG, Zhai FG, et al. Electromagnetic Characteristics Analysis and Structure Optimization of High-Speed Fuel Electromagnets. Machines. 2022; 10: 964.
- 22. Hong YS, Kwon YC. Electromagnetic Analysis of a Flat-Type Proportional Solenoid by the Reluctance Method. Int. J. Precis. Eng. Manuf. 2006; 7: 46–51.
- 23. Yu YX, Ke SD, Jin KD. Structural parameters optimization for a proportional solenoid. Int. J. Simul. Model. 2020; 19: 689–700.
- 24. Liu P, Ouyang YW, Quan WW. Multi-objective optimization of a long-stroke moving-iron proportional solenoid actuator. Micromachines. 2024; 15: 58.
- 25. Tang JH, Zuo YY. The Design and Magnetic Field Analysis of a Double Rotor Permanent Magnet Braking Device. Processes. 2022; 10: 346.
- 26. Wang YB, Chu L, Ma WT, Cai JW, Bai GJ. Research on Hydraulic Response Characteristics of Inlet Valve Used in Hydraulic Braking System. Appl. Mech. Mater. 2014; 2963: 175–179.